# The Emplacement mechanism of Bouin-Miandasht granitoid pluton(Sanandaj- Sirjan zone, West Iran): An application of AMS method

Soheila Saki[1]*, Mahmoud Sadeghian[1]

1- Department of Geology, Faculty of Sciences, Shahrood University of Technology, Shahrood, Iran.

* Corresponding Author: s.saki1390@yahoo.com

*Received: 06 May 2014 / Accepted: 12 November 2014 / Published online: 19 November 2014*

## Abstract

Bouin- Miandasht Granitoid Pluton (BMGP), which outcropped to the north of Bouin-Miandasht-Aligoudarz road, was emplaced into low to medium grade of Triassic to early Jurassic metapelitic rocks of Sanandaj-Sirjan Structural Zone. In this study we do provide the first investigations of BMGP by means of anisotropy of magnetic susceptibility (AMS). Most Km values for the main felsic compositions of this pluton are lower than 500 µSI, suggesting it belongs to paramagnetic granites. Felsic part suffered high temperature solid state deformation during emplacement and show magmatic microstructures. The pluton also show low temperature solid state microstructures; which are related to later compressional tectonic regimes. Low plunge magnetic lineations together with low dip foliations defined on the base of magnetic parameters point out that the Bouin-Miandasht granitoid pluton was emplaced as a large sill in a dextral shearing zone related to a transpressional regime.

**Keywords:** AMS; Magnetic parameters; Microstructures; Emplacement mechanism; Bouin-Miandasht; Sanandaj-Sirjan.

## 1–Introduction

The internal structures of granite plutons are known for several decades to be remarkably regular in orientation, at least for their planar fabrics (Cloos, 1931). Many structural studies have used this property to unravel the emplacement and/or deformational history of plutons (e.g., Cloos, 1932; Bouchez *et al*., 1981; Guineberteau *et al*., 1987). Magnetic fabrics have been used since the work of Graham (1954) to decipher mineral and deformation fabrics in rocks. Measurements of magnetic fabrics are not only easier, more precise and more reproducible than optical methods, but also allow lineations to be defined, giving an invaluable element for kinematic and geodynamical reconstructions (Balsley and Buddington, 1960; Bouchez *et al*., 1990; Bouchez, 1997).

Magnetic fabric analysis is a powerful approach for studying granites because it provides magmatic to strain patterns at a regional scale, in rocks where fabric is difficult to characterize (e.g. Bouchez, 2002). Ascent and emplacement of granitic magmas have been the subject of a lively debate in the last decade (Benn *et al*., 1998; Clemens, 1998).

Magnetic fabrics have long been considered as proxies for mineral fabrics in a wide range of rocks (Hrouda 1982; Rochette *et al*. 1992; Tarling and Hrouda 1993; Borradaile and Henry 1997). The success of magnetic fabric methods lies in their ability to measure the orientation of hundreds of grains within minutes, as opposed to the universal stage or electron backscattered diffraction methods.

*Table 1) Some reported geochronological ages of SSZ plutonic rocks. (after Ahadnejad et al., 2011).*

| **Area** | **Rocks** | **Method** | **Sr$_{(initial)}$** | **Age (Ma)** | **References** |
|---|---|---|---|---|---|
| Urumieh | fluorite alkali granite | K-Ar | | 76.6 ± 3.4 | Ghalamghash *et al*., 2009 |
| | alkali granite | K-Ar | | 80.1 ± 3.1 | |
| | diorite | K-Ar | | 93.0 ± 2.3 | |
| Pichagchi | Tonalite | K-Ar | | 74.2 | Kholghi khasraghi and Vossoughi Abedini, 2004 |
| | Diorite | K-Ar | | 74.2 | |
| | Granodiorite | K-Ar | | 74.2 | |
| | | K-Ar | | 74.2 | |
| | Quartz diorite | K-Ar | | 116.02 | Kholghi khasraghi, 1999 |
| Almogholagh | Diorite | Rb-Sr | 0.708 | 144±17 | Valizadeh and Cantegral, 1975 |
| Alvand | Norite | Rb-Sr | 0.708 | 78-89 | |
| | Norite | K-Ar | 0.708 | 89.1±3 | |
| | Pegmatite | Rb-Sr | | 104±3 | |
| | Pegmatite | K-Ar | | 82.8±3 | |
| | Porphyroid Granite | Rb-Sr | 0.709 | 68±2 | |
| | Porphyroid Granite | K-Ar | | 63.8-80.8±3 | |
| | Porphyroid Granite | K-Ar | | 64±2 | Braud, 1987 |
| | Porphyroid Granite | K-Ar | | 81.8±1.9 | Baharifar *et al*,. 2004 |
| | Pegmatite | K-Ar | | 74.7±1.8 | |
| | Diorite | K-Ar | | 135.2±3.1 | |
| | Quartz Diorite | K-Ar | | 73.2±3.1 | |
| | | | | Middel Jurassic | Shabazi (in Ghalamghash *et al.,* 2009) |
| Astaneh | Diorite | Rb-Sr | 0.710 | 98.9±1.5 | Masoudi, 1997 |
| Boroujerd | Granite | Rb-Sr | 0.707 | 60±0.7 | |
| | Granite | Rb-Sr | 0.709 | 70±0.7 | |
| | Pegmatite | Rb-Sr | 0.708 | 52±.0.5 | |
| | Granite | Rb-Sr | 0.709 | 130±1.4 | |
| | Diorite | Rb-Sr | 0.706 | 117.2±1.2 | |
| | Pegmatite | Rb-Sr | 0.738 | 127.3±1.3 | |
| | Pegmatite | Rb-Sr | 0.743 | 119.2±1.3 | |
| | Quartz Diorite | U-Pb | | 170.7±1.6 | Ahmadi-Khalaji *et al.,* 2007 |
| | Granodiorite | U-Pb | | 169.6±0.2 | |
| | Granodiorite | U-Pb | | 171.3±1.1 | |
| | Granodiorite | U-Pb | | 170.7±1 | |
| | Monzogranite | U-Pb | | 171.7±1.5 | |
| | Pegmatite | U-Pb | | 170.7±1.5 | |
| Malayer | Granodiorite | U-Pb | | 187±6 | Ahadnejad *et al*., 2011 |
| | Granodiorite | U-Pb | | 170±4 | |
| | Monzogranite | U-Pb | | 174±6 | |
| | Monzogranite | U-Pb | | 162±8 | |
| | Syenogranite | U-Pb | | 183±5 | |
| | Syenogranite | U-Pb | | 174±5 | |
| | Tonalite | U-Pb | | 169±8 | |
| | Quartz Diorite | U-Pb | | 172±2 | |
| Aligoodarz | Granite | U-Pb | | Middel Jurassic | Asnaashry, 2009 |

The anisotropy of magnetic susceptibility (AMS) measured in low field has been proven to be particularly useful for studying the flow of igneous rocks (e.g. Cañón-Tapia *et al*., 1996;

Bouchez, 1997). In the recent years, the measurement of anisotropy of magnetic susceptibility (AMS) has been used as a tool to analyze fabrics in variety rocks and materials (e.g., Hrouda, 1982; Tarling and Hrouda, 1993; Borradaile and Henry, 1997; Ferre *et al*., 2004; Borradaile and Jackson, 2004).

Khan (1962) presented the first interpretation of AMS in igneous rocks and dykes and the technique has been used since then in order to understand lava flow and emplacement mechanism of igneous rocks (Hargraves *et al*., 1991; Tauxe *et al*., 1998). Many authors recognized that tectonics often controls magma emplacement, especially in shear zones (e.g. Hutton *et al*., 1990; D'Lemos *et al*., 1992; Hutton and Reavy, 1992). In the absence of direct geochronological evidence, correlating the deformations and the mode of emplacement of granite bodies with regional tectonic events is a challenge because granitic rocks do not always display deformation fabrics at a mesoscopic scale. Anisotropy of magnetic susceptibility (AMS) studies may be used to characterize and measure weak anisotropic fabrics (foliations and lineations), either magmatic or solid-state ones, which are essential to describe the different deformations for a granite, to identify the constraints leading to the granite intrusion, and finally to link these features to the regional tectonics.

Microstructural and AMS data were gathered, described and analyzed to infer emplacement and tectonic relationships for these granites. The AMS technique can be used to study magma emplacement mechanisms, and it has been shown to be a powerful tool that allows us to infer both the direction of magma flow and the location of its source (Zhang *et al*., 2011).

## 2-Geological setting

From Late Precambrian until Late Paleozoic time, southeastern Turkey, central Iran and Arabia were part of the NE Gondwana continent, separated from the Eurasian plate by the Paleo-Tethys Ocean. The closure of Paleo-Tethys during Upper to Lower Triassic time by the northward motion of the Central Iran microcontinents resulted in their welding with the Eurasian plate along Paleo-Tethys remains consisting of oceanic rocks. Rifting along the present Zagros fold and thrust belt of the continental plate took place in the Permian to Triassic, resulting in the opening of the Neo-Tethys Ocean. The onset of the progressive subdaction of the Neo-Tethys Ocean may have taken place as late Triassic up to Middle Jurassic (c. 170 Ma), when a new northward subduction beneath the Sanandaj–Sirjan block formed (Berberian and King, 1981; Masoudi, 1997).

The Sanandaj-Sirjan Zone is a metamorphic belt in the N-NE part of the Zagros fold and thrust belt caused by the convergence of the Afro-Arabian continent and the Iranian micro continent during the Late Cretaceous-Miocene (Mohajjel *et al*., 2003). This zone is one of the most dynamic structural zones of Iran which experienced complex protracts Late Precambrian to Tertiary evolution (Moritz *et al*., 2006). The SSZ extends for 1500 km along strike from northwest (Sanandaj) to southeast (Sirjan) in the western part of Iran and has a width of 150-200 km (McCall 2002). The orogenic belt is the result of closure of Neo Tethys by consumption of oceanic crust at a northeast dipping subduction zone below central Iran and subsequent late Cretaceous continental collision between the Afro-Arabian and Iranian continental fragments (Mohajjel *et al*., 2003; Agard *et al*., 2005; Ghasemi and Talbot, 2006). The Sanandaj–Sirjan Zone contains the metamorphic core of the Zagros continental collision zone in western Iran, and is divided into an outer belt of imbricate thrust slices that includes the Zagros suture and an inner belt of mainly Mesozoic metamorphic rocks (Mohajjel *et al*., 2003). Detailed mapping in the northwestern part of the Sanandaj–Sirjan Zone has delineated the complex structural history of these rocks (Mohajjel and Fergusson, 2000). In addition, In the Golpaygan area, The SSZ is subdivided into two parts (Eftekharnejad, 1981): (i) the southern part (South SSZ) consists of rocks deformed and metamorphosed in Middle to Late Triassic; and (ii) the northern part (North SSZ), deformed in the Late Cretaceous, contains many intrusive felsic rocks (such as the Alvand, Boroujerd, ,bouin- miandasht and Malayer plutons, Ghasemi and Talbot, 2006) (Fig. 1).

The Bouin-Miandasht granitoid pluton emplaced into low to medium grade of Triassic to early Jurassic metapelitic rocks of SSZ. The pluton has a bimodal composition including mantle (gabbro – diorites) and crustal (alkali feldspar – leucogranites) end members. On the base of field relations, previous authors (e.g. Ghasemi, 1992) suggest that the emplacement of the pluton with in the metamorphic rocks caused contact metamorphism at ~70 Ma during the Laramide orogeny. However, recent workers (e.g. Ahmadi Khalaji *et al.*, 2007; Ahadnejad *et al.*, 2011) obtained an age of 170 Ma for some of the similar history plutons of SSZ, these plutons might be formed during Cimmerian orogeny. The Table 1shows some of the obtained new age intermediations of granitoid plutons of North part of Sanandaj–Sirjan structural zone. The obtained ages all of the refer to big magmatism event in Middle Jurassic.

## 3-Methods and sampling

More than 225 oriented specimens were collected for the AMS investigation from 65 stations within Bouin- Miandasht granitoid pluton. Drilling was done in 65 stations from different lithological units of the granitoid pluton (Fig. 2). Sampling at each site was performed with a portable drilling machine. At each station, at least two cores were drilled which have 25mm in diameter and at least 5 cm longs, Cores were cut into 2 to 7 cylindrical specimens with 22 mm in height. AMS measurements was performed with a MFK1-FA Kappabridge susceptometer of Agico Ltd (Brno, Czech Republic) and have a sensitivity of (about $2 \times 10^{-8}$ SI) in geomagnetic laboratory of earth science faculty of Shahrood University.

The anisotropy of magnetic susceptibility (AMS) is described mathematically as a symmetrical second rank tensor, which can be visualized as an ellipsoid with three principal axes including maximum (K1), intermediate (K2), and minimum (K3) susceptibility. The long axis is normally referred to the magnetic lineation and the short axis to the pole of magnetic foliation plane (Tarling and Hrouda, 1993). Stereogram position of the three axis magnetic elliptical K1, K2 and K3 in different rocks from study area shown in Figure 3.

The mean susceptibility K mean is the mean value of the magnitudes for three axes of the AMS ellipsoid: K mean = $(K_1+K_2+K_3)/3$. Two parameters, the corrected anisotropy degree (P') and the shape parameter (T), were used to describe the intensity and character of the magnetic fabric (Jelínek, 1981; Tarling and Hrouda, 1993):

$$P'=\exp\{2[(\ln K_1-\ln K_m)^2+(\ln K_2-\ln K_m)^2+(\ln K_3-\ln K_m)^2]\}^{1/2}$$

$$T=2\ln(k_2/k_3)/\ln(k_1/k_3)-1$$

## 4-Results

### 4.1- Magnetic susceptibility data

The geographical locations and the magnetic data for all the sampling stations from the BMGP are reported in the Table 2. The measured mean magnetic susceptibility values (Km in µSI) of the different rock types of the BMGP are as follows: gabbro – diorites (769), alkali feldspar granites (158), granites (133) (includes of fine granites (120), coarse granites (166)), leucogranites (34). The Kmvalues for the main rock types, are lower than 500 µSI (Fig. 4) representing that this pluton belongs to paramagnetic granites. Biotite has the most important role for magnetic properties of BMGP (Saki, 2014).

*Table 2) Data obtained from measuring the magnetic fabric in BMGP.*

| Station | X | Y | Lithology | $K_m$ | $K_1d$ | $K_1i$ | $K_3d$ | $K_3i$ | P%=( P-1).100 | T |
|---|---|---|---|---|---|---|---|---|---|---|
| SS-1 | 425890 | 3667240 | A F G | 107 | 3 | 17 | 253 | 49 | 6.1 | 0.53 |
| SS -2 | 426223 | 3665377 | C G | 155 | 196 | 5 | 289 | 35 | 4.5 | 0.47 |
| SS -3 | 425608 | 3665885 | A F G | 129 | 173 | 35 | 290 | 33 | 2.7 | 0.49 |
| SS -4 | 425966 | 3665836 | C G | 200 | 194 | 15 | 300 | 46 | 2.9 | 0.46 |
| SS -5 | 426083 | 3666025 | A F G | 183 | 198 | 25 | 316 | 45 | 5.7 | 0.42 |
| SS -6 | 426436 | 3664973 | C G | 161 | 192 | 18 | 295 | 34 | 5.6 | 0.45 |
| SS -7 | 426002 | 3665299 | A F G | 166 | 191 | 29 | 317 | 46 | 3.3 | 0.54 |
| SS -8 | 425715 | 3665601 | " | 136 | 170 | 35 | 306 | 46 | 3.9 | 0.33 |
| SS -9 | 425669 | 3665286 | " | 143 | 190 | 34 | 315 | 54 | 3.1 | 0.09 |
| SS -10 | 424545 | 3665696 | " | 124 | 174 | 16 | 288 | 56 | 1.6 | -0.09 |
| SS -11 | 425779 | 3666962 | LG | 47 | 28 | 18 | 261 | 65 | 5.6 | 0.59 |
| SS -12 | 425358 | 3666931 | A F G | 134 | 9 | 11 | 274 | 24 | 6.2 | 0.46 |
| SS -13 | 425095 | 3666287 | " | 141 | 163 | 36 | 282 | 34 | 2.3 | -0.02 |
| SS -14 | 425466 | 3665813 | " | 122 | 188 | 29 | 294 | 27 | 2.3 | 0.41 |
| SS -15 | 425628 | 3665720 | " | 133 | 174 | 42 | 300 | 33 | 3.3 | 0.14 |
| SS -16 | 425687 | 3665648 | " | 137 | 182 | 36 | 305 | 37 | 3.3 | 0.72 |
| SS -17 | 424645 | 3666129 | " | 118 | 180 | 12 | 275 | 23 | 1.5 | -0.43 |
| SS -18 | 422824 | 3665914 | F G | 122 | 74 | 35 | 247 | 55 | 2.5 | 0.53 |
| SS -19 | 424461 | 3666431 | A F G | 120 | 172 | 5 | 263 | 11 | 2.0 | -0.31 |
| SS -20 | 424270 | 3666215 | " | 157 | 185 | 24 | 93 | 5 | 2.2 | 0.13 |
| SS -21 | 423328 | 3666786 | C G | 132 | 211 | 14 | 315 | 44 | 1 | 0.56 |
| SS -22 | 423419 | 3666841 | Gb -Di | 652 | 337 | 30 | 197 | 53 | 0. 6 | 0.15 |
| SS -23 | 422824 | 3666501 | F G | 116 | 175 | 11 | 72 | 50 | 2.2 | 0.08 |
| SS -24 | 422672 | 3666697 | " | 117 | 338 | 25 | 237 | 23 | 1. 2 | -0.04 |
| SS -25 | 421528 | 3667453 | " | 133 | 193 | 9 | 63 | 76 | 2.7 | 0.50 |
| SS -26 | 422058 | 3667677 | Gb -Di | 110 | 26 | 25 | 164 | 58 | 3.1 | -0.007 |
| SS -27 | 421559 | 3667967 | " | 545 | 195 | 12 | 103 | 10 | 0. 6 | 0.51 |
| SS -28 | 422021 | 3670839 | A F G | 180 | 175 | 31 | 291 | 36 | 4.3 | 0.60 |
| SS -29 | 421763 | 3670276 | " | 300 | 156 | 9 | 248 | 12 | 7.7 | 0.06 |
| SS -31 | 420590 | 3670676 | LG | 50 | 0 | 34 | 106 | 22 | 2.6 | -0.09 |
| SS -32 | 420704 | 3671033 | A F G | 188 | 19 | 27 | 151 | 53 | 3.9 | 0.11 |
| SS -33 | 420984 | 3671258 | " | 475 | 150 | 0.5 | 246 | 85 | 7.2 | -0.08 |
| SS -34 | 421310 | 3671308 | " | 117 | 157 | 14 | 254 | 43 | 9.5 | 0.24 |
| SS -35 | 421538 | 3671422 | " | 124 | 13 | 60 | 166 | 27 | 3.7 | 0.50 |
| SS -36 | 421506 | 3671045 | " | 288 | 146 | 17 | 253 | 44 | 12 | 0.31 |
| SS -37 | 421524 | 3670703 | " | 184 | 332 | 16 | 225 | 48 | 4.3 | 0.17 |
| SS -38 | 421489 | 3670418 | " | 149 | 12 | 19 | 242 | 62 | 4.2 | 0.08 |
| SS -39 | 421303 | 3670231 | " | 135 | 142 | 17 | 247 | 40 | 2.2 | -0.18 |
| SS -40 | 422153 | 3669521 | F G | 68 | 22 | 37 | 155 | 43 | 2.3 | 0.06 |
| SS -41 | 422266 | 3669573 | " | 90 | 344 | 18 | 225 | 56 | 13.5 | 0.49 |
| SS -42 | 422415 | 3669633 | " | 98 | 325 | 37 | 127 | 52 | 15 | -0.13 |
| SS -43 | 422459 | 3669581 | " | 101 | 10 | 26 | 217 | 62 | 3.9 | 0.49 |
| SS -44 | 420067 | 3671898 | " | 121 | 57 | 16 | 196 | 69 | 8.3 | 0.50 |
| SS -45 | 420051 | 3671752 | " | 107 | 31 | 20 | 170 | 65 | 7.9 | -0.05 |
| SS -46 | 420160 | 3671504 | A F G | 152 | 32 | 20 | 266 | 58 | 4.6 | 0.76 |
| SS -47 | 420472 | 3671044 | " | 122 | 20 | 17 | 231 | 71 | 13 | 0.26 |
| SS -48 | 420611 | 3671212 | " | 122 | 177 | 14 | 301 | 67 | 8.5 | 0.13 |
| SS -49 | 420288 | 3670936 | " | 144 | 25 | 18 | 190 | 72 | 3.2 | 0.30 |
| SS -50 | 420288 | 3670936 | " | 120 | 28 | 19 | 220 | 71 | 4.3 | -0.17 |
| SS -51 | 419978 | 3671499 | " | 136 | 28 | 14 | 273 | 59 | 3.4 | 0.28 |
| SS -52 | 419564 | 3671702 | F G | 107 | 310 | 2 | 213 | 75 | 7.5 | 0.85 |
| SS -53 | 419690 | 3671466 | A F G | 129 | 28 | 15 | 266 | 62 | 3 | 0.51 |
| SS -54 | 422813 | 3670127 | C G | 183 | 32 | 15 | 283 | 51 | 3.6 | 0.53 |
| SS 55a | 422730 | 3670242 | LG | 5 | 333 | 16 | 310 | 8 | 10 | 0.002 |

| | | | | | | | | | | |
|---|---|---|---|---|---|---|---|---|---|---|
| SS55 b | 422716 | 3670232 | A F G | 149 | 13 | 21 | 268 | 35 | 4.5 | 0.27 |
| SS -56 | 422639 | 3670393 | " | 421 | 12 | 10 | 266 | 57 | 8.7 | 0.48 |
| SS -57 | 422402 | 3670282 | " | 139 | 345 | 6 | 247 | 55 | 3.1 | 0.34 |

*Table 2) Continued*

| Station | X | Y | Lithology | Km | K1d | K1i | K3d | K3i | P%=( P-1).100 | T |
|---|---|---|---|---|---|---|---|---|---|---|
| SS -58 | 422541 | 3670138 | F Gr | 254 | 62 | 3 | 323 | 68 | 2.4 | 0.17 |
| SS -59 | 423937 | 3668990 | A F G | 160 | 10 | 20 | 261 | 43 | 5.8 | 0.51 |
| SS -60 | 423756 | 3668441 | " | 120 | 0.4 | 0.3 | 269 | 79 | 5.4 | 0.53 |
| SS -61 | 423414 | 3668687 | " | 114 | 157 | 14 | 264 | 48 | 4.8 | 0.45 |
| SS -62 | 423308 | 3668602 | " | 112 | 152 | 29 | 269 | 38 | 5.9 | 0.03 |
| SS -63 | 423417 | 3668382 | " | 113 | 165 | 27 | 270 | 26 | 3.8 | 0.37 |
| SS -64 | 424228 | 3668231 | " | 115 | 25 | 12 | 290 | 25 | 5 | 0.53 |
| SS -65 | 424537 | 3668095 | " | 129 | 19 | 12 | 276 | 47 | 9 | 0.46 |
| SS -66 | 423700 | 3667975 | " | 115 | 180 | 3 | 275 | 62 | 3.2 | 0.43 |

** AFG: Alkali Feldspar Granite, CG: Corse grain Granit, LG: leucogranite, FG: Fine grain Granite, Gb- Di: Gabbro- Diorite.*

## 4.2- AMS directional data

The orientation data from the AMS measurements were used to build up the structural maps in (Figs. 5 and 6). The general trend of magnetic lineations of this pluton is North-South and the strike of the magnetic foliation is East–West.

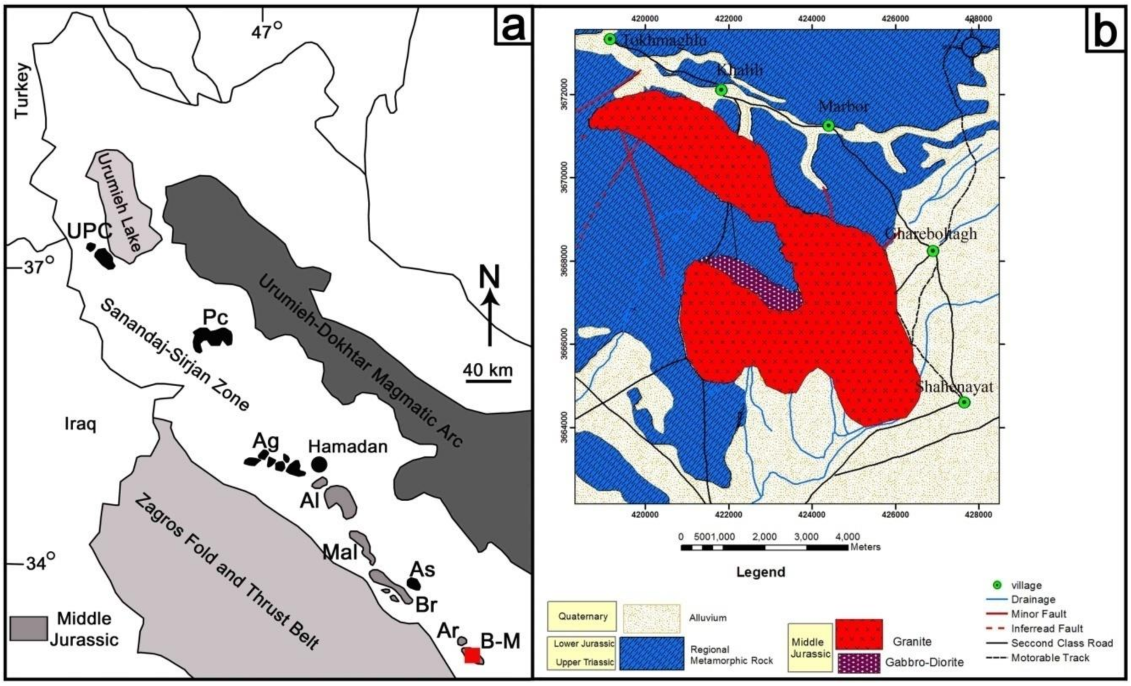


*Figure 1a) Location map of the study area in Sanandaj–Sirjan zone; (UPC = Urumieh plutonic complex, PC = Pichagchi, AG = Almogholgh, AL = Alvand, Mal = Malayer, Br = Boroujerd, AS = Astaneh, Ar = Aligudarz, BM= Bouin_ Miandasht) after Ahadnejad et al., 2011), b) Geological map of the BMGP.*

The average magnetic lineations is183º/04º and the average pole of the magnetic foliation is 268º/54º.However, in N–NW areas which has been affected by compressional tectonic regimes, show turbulent and disordering magnetic foliations and lineations. Intensive deformation in the N–NW of the region can be attributed to shear zones and faulting.

## 4.3-AMS scalar data

The percentage of magnetic anisotropy (P%) varies from 1 to 15. Gabbro – diorites and alkali feldspar granites have the maximum and minimum values of (P%), in respectively and show positive correlation with degree of deformation (Fig. 7). Shape parameter (T) values varies from -0.43 to 0.85 and most of the magnetic ellipsoids are oblate (Fig. 8). in felsic parts Seventy five percent of specimens have positive T. This subject indicates that magnetic ellipsoids are oblate and then foliation is prevailing, field evidence confirms this conclusion. Magnetic behavior of compositional rock groups of this pluton confirms the bimodal composition of it.

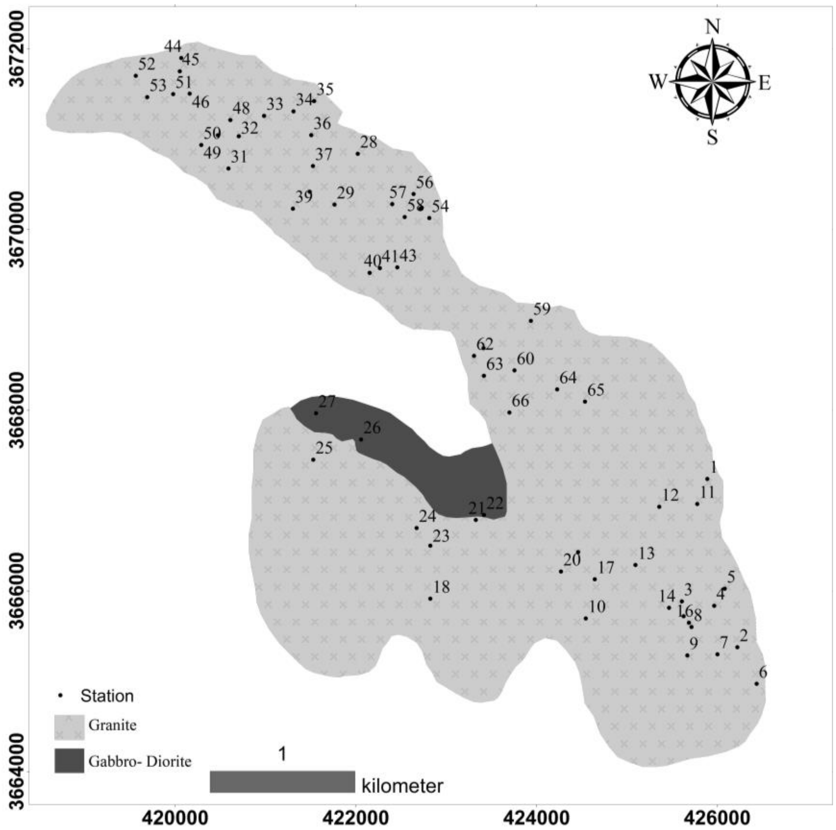


*Figure 2) Distribution of sampling sites in the BMGP.*

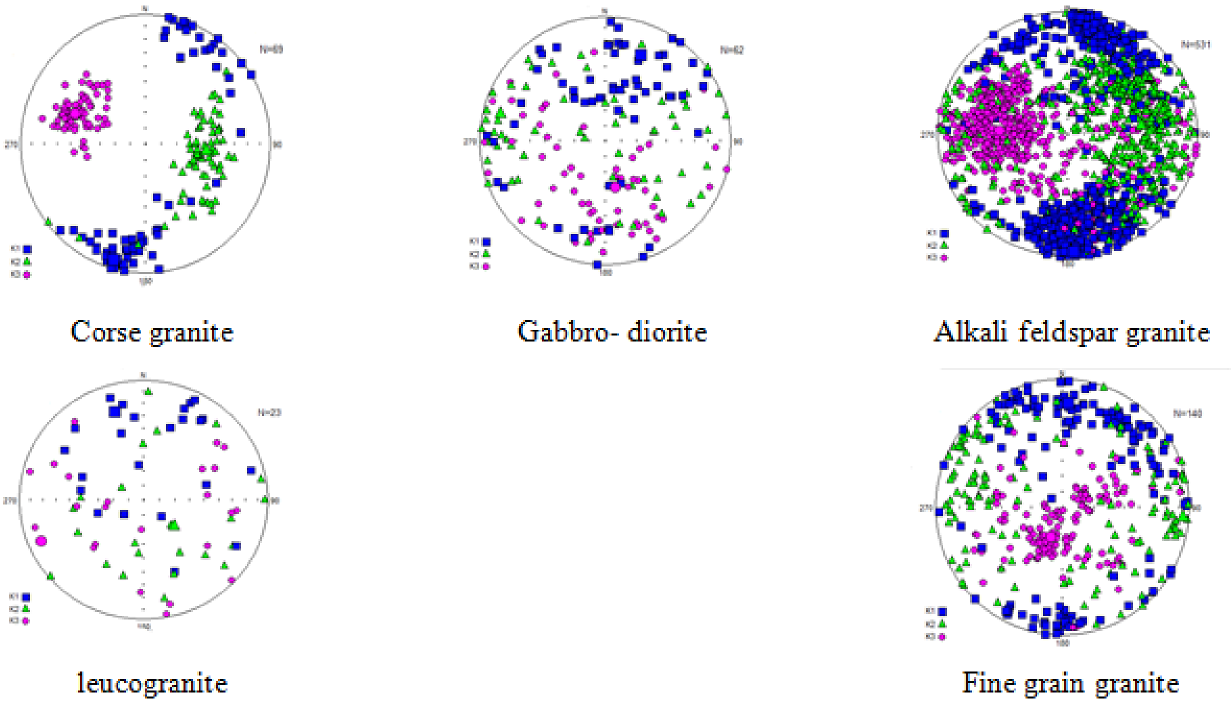


*Figure 3) Streogram of magnetic axis position from various rocks in the study area.*

Arrangement of K feldspar megacryst elong the foliation it possible to see in figures 9a and b). elongations and arrangment of metapelitic enclaves in BMGP as it possible to see, metapelitic enclaves arranged parallel to N–S line (Figs. 9c, d). This observation is compatible to magnetic foliations. a major foliation in the field (Fig. 10) and obtained magnetic foliation confirmed another.

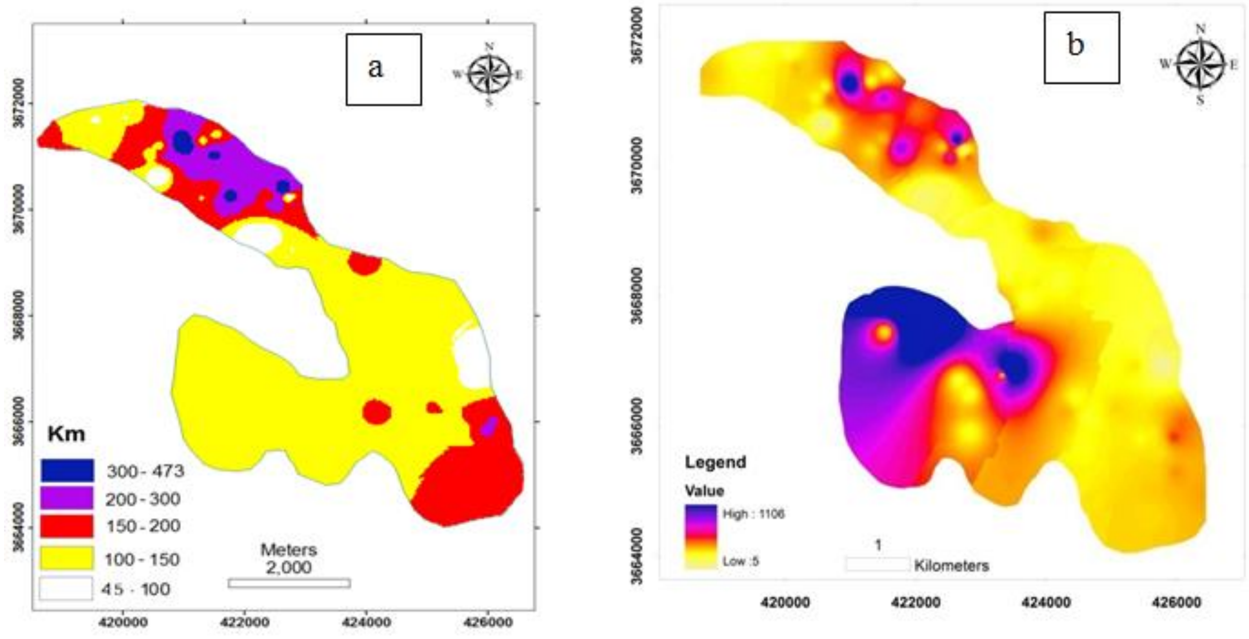


*Figure 4) Contour maps of the Km from the BMGP: a) felsic part, b) mafic and felsic.*

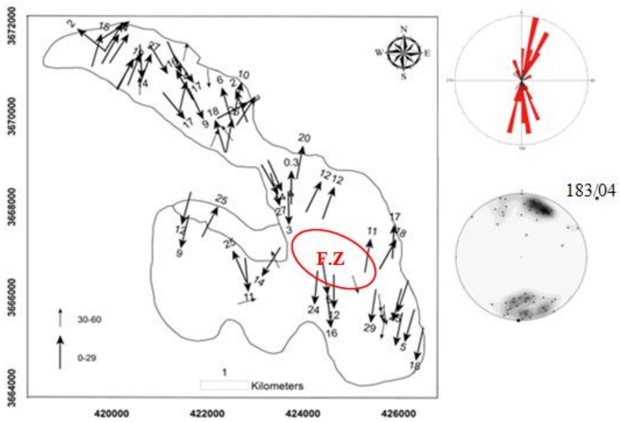


*Figure 5) The magnetic lineation map of study area. F.Z: feeder zone.*

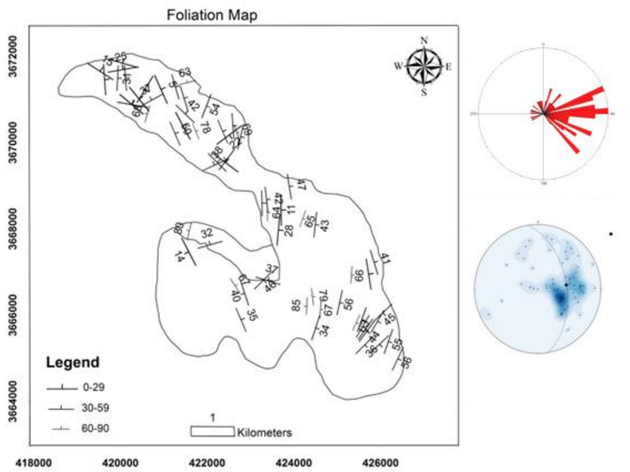


*Figure 6) Magnetic foliation map of BMGP.*

### 4.4-Microstructural data

In granitic rocks, the microstructures provide useful indications about the physical state of magma at the time of acquisition of its fabric and, eventually, and about suffered the solid-state overprints. Previous workers (e.g. Paterson *et al*., 1989; Bouchez *et al*., 1990) defined microstructural criteria, essentially based on the observation of quartz, feldspar and biotite.

An accurate interpretation of the internal structures of a pluton requires a detailed study of its microstructures in order to determine if the deformation took place in the magmatic state or in the solid state (high or low temperature). In accordance with several other studies dealing with the microstructures present in granitic rocks (Bouchez *et al*., 1981; Paterson *et al*., 1989), the following types of microstructures are defined.

Detailed study of more than 115 thin sections, which were prepared from the specimens used for the AMS study. This study, helped us to recognize the following subjects: (1) magmatic microstructures are present in most parts of the pluton; (2) sub- magmatic microstructures that manifested by fractured K feldspar infilled by quartz, have been seen in the north, northwest and to a lesser extent in the southern part; (3) the high temperature solid state sub solidus microstructures have less abundance than other microstructures in the pluton; (4) low temperature solid state microstructures can been observed in the pluton contacts with country rocks specially at N and NE margins; (5) mylonites are present in the north and north-west margins (Figs. 11 and 12). The deformation rate in N and NW parts of the pluton can be attributed to shear zones and faults (Fig. 13). High-temperature solid state and magmatic microstructures occurred during pluton emplacement, and the low-temperature solid-state microstructures most probably took place after pluton emplacement in the studied rocks caused by later compression tectonic regimes.

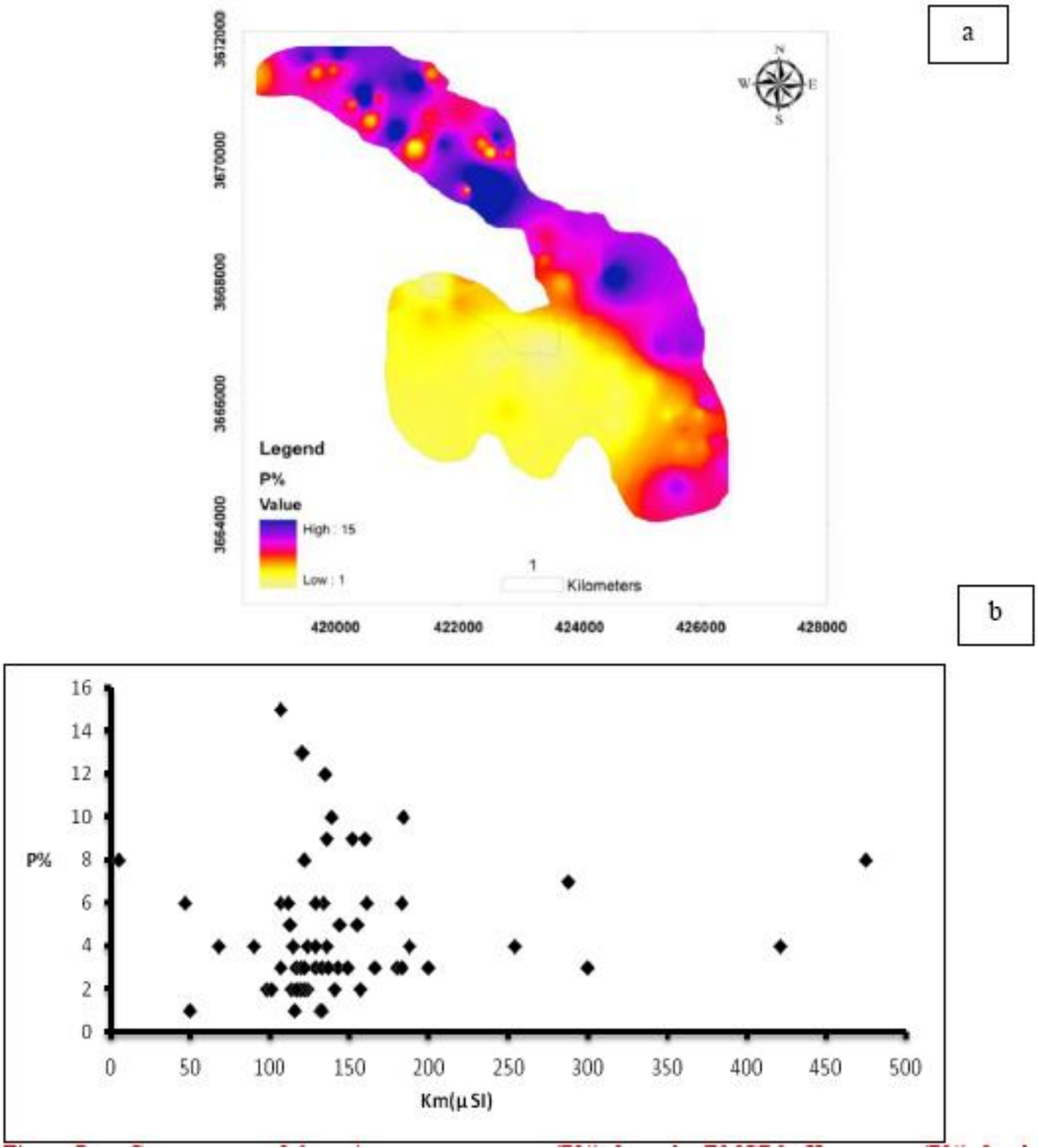


*Figure 7. a, Contour map of the anisotropy percentage (P%) from the BMGP.b, Km versus (P%) for the BMGP.*

## 5-Discussion

### 5.1- Dividing the pluton into domains

On the basis of the microstructural observations, the magnetic foliation and lineation, bulk susceptibility, P, T and lithological maps, four main structural domains were distinguished in the Bouin- Miandasht pluton, including: A, B, C and D. The A domain is subdivided into two sub-domains; and B domain is subdivided into three sub-domains. Domains C and D are not divided. The D domain includes gabbro–dioritic rocks.

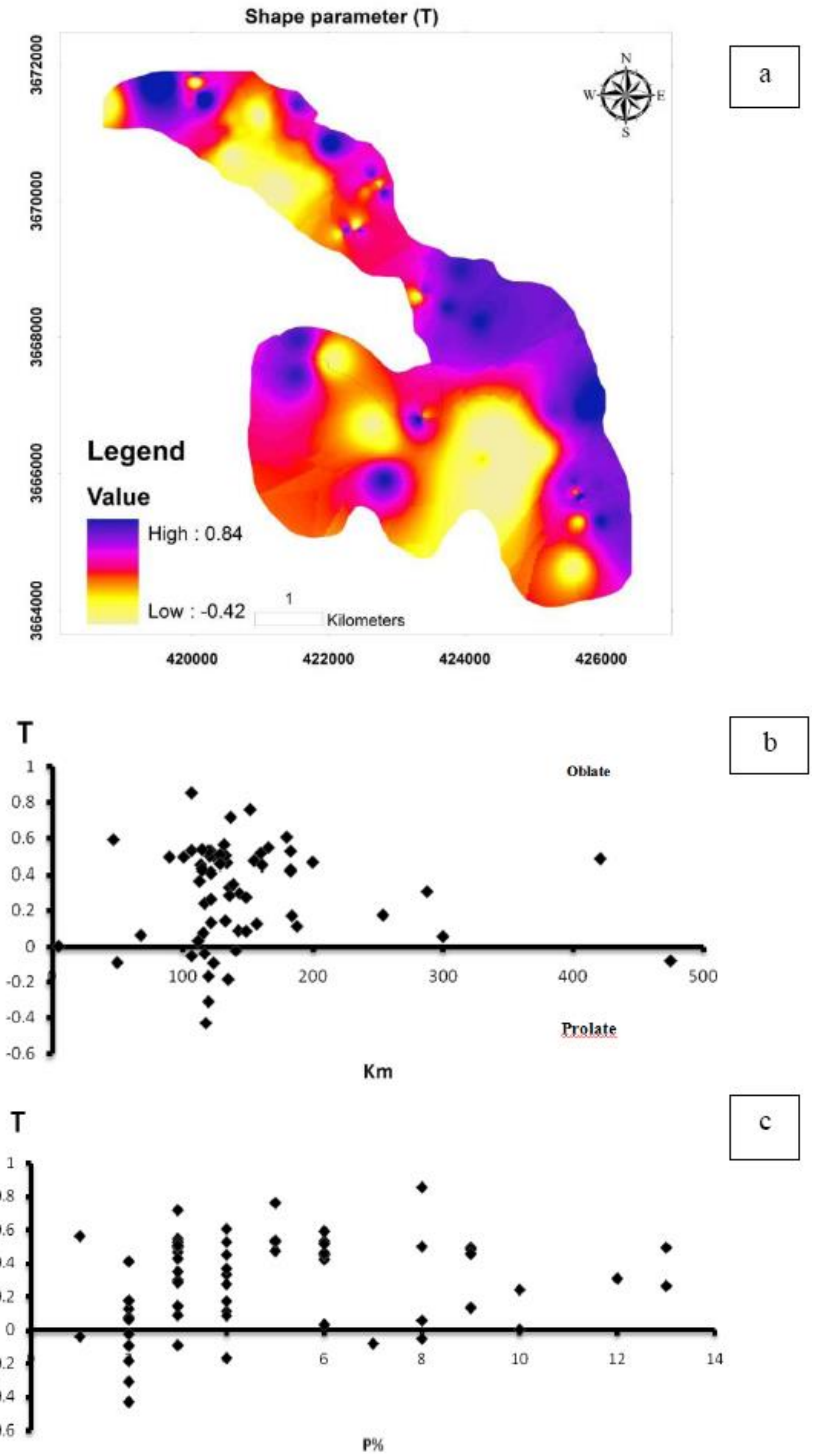

*Figure 8a) Contour map of the shape parameter (T) from the BMGP.b) Km versus (T) and c) Anisotropy percentage (P%) versus shape parameter (T) for the BMGP.*

### 5.1.1-A Domain

According to trends and plunges of lineation, we divided this domain into two subdomains. The fabric pattern of this unit shows N–S lineation, with mean at 183º/18º and the best pole of foliation is 284°/39° (Fig. 14).

*A1 Subdomain (7 stations*)

The lithological composition of six stations from this subdomain is alkali feldspar granite, and the other is leucogranite. Subdomain A1 has magmatic to submagmatic microstructures in most stations; but one of the stations which located at the margin of the pluton shows low temperature solid state microstructures. The fabric pattern of this unit shows N–S lineation, with mean at 011º/12º and the best pole of foliation has mean at 272°/44° (Fig. 15). The highest and lowest susceptibility Km valuse are 160 and 47 μSI, respectively (average at 116 μSI). P% values range from 0.5 to 9 and the shape parameter (T) of these subdomains is oblate with T values range from 0.45–0.59.

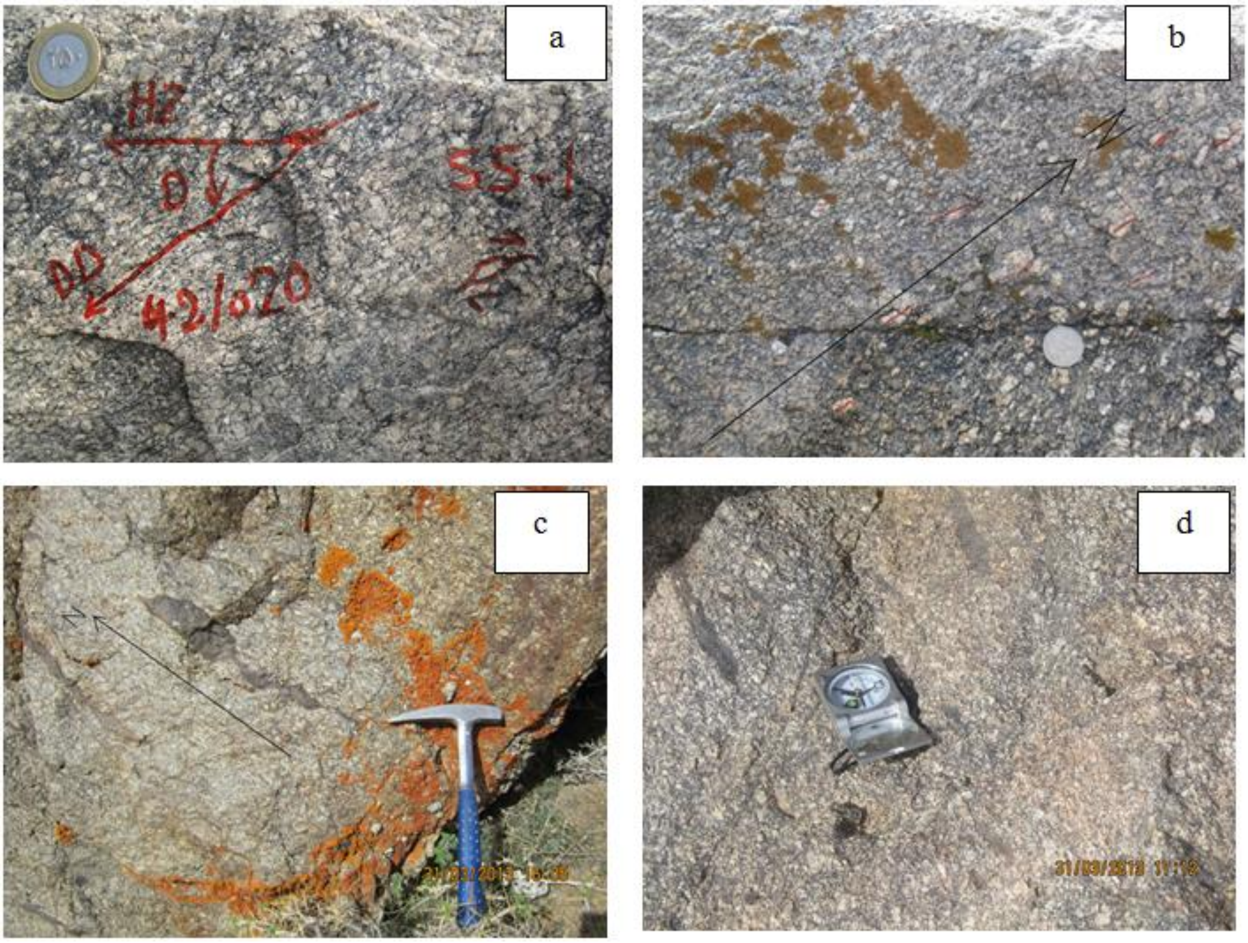


*Figure 9a and b) Arrangement of K feldspar megacryst elong the foliation, c and d) elongations and arrangment of metapelitic enclaves parallel to N- S line in BMGP.*

*Subdomain A2 (feeder zone: 21 stations)*

It is located in the southern part of pluton and mostly corresponds to alkali feldspar granites and coarse grain granitic rocks with magmatic and submagmatic microstructures. The lineations of this subdomain have steeply plunges (181°/23°), suggesting that it might be a feeder zone. The best pole of foliation of subdomain A2 is 290°/38° (Fig. 15). The average susceptibility is 128 μSI, and the P% values range from 0.9 to 5.9 percent. The shape parameter (T) for seventeen stations of subdomain A2 is oblate and for four stations is prolate with T-values range from -0.430 to 0.716.

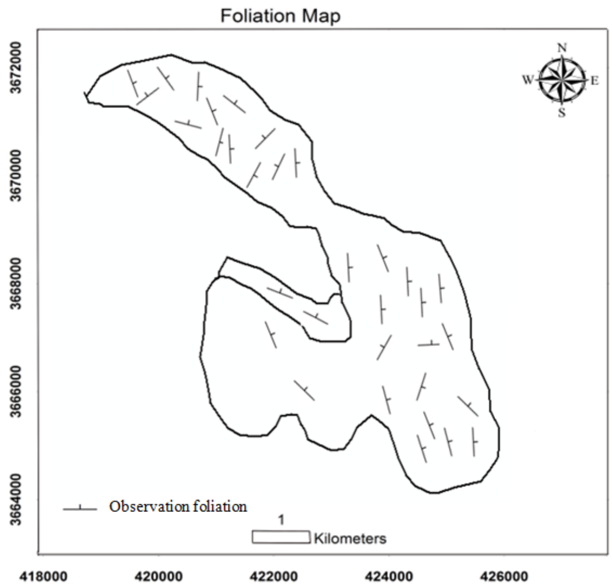


*Figure 10) Observed foliation in the field from the BMGP.*

### 5.1.2-B Domain

Domain B is also a major part of this pluton (30 stations). According tolineation and foliation trends, it can be subdivided into three subdomains: B1, B2, B3. The lineations of domain have mean trend/plunge at 005°/14°, and the best pole of foliation has mean at 237°/65° (Fig. 16).

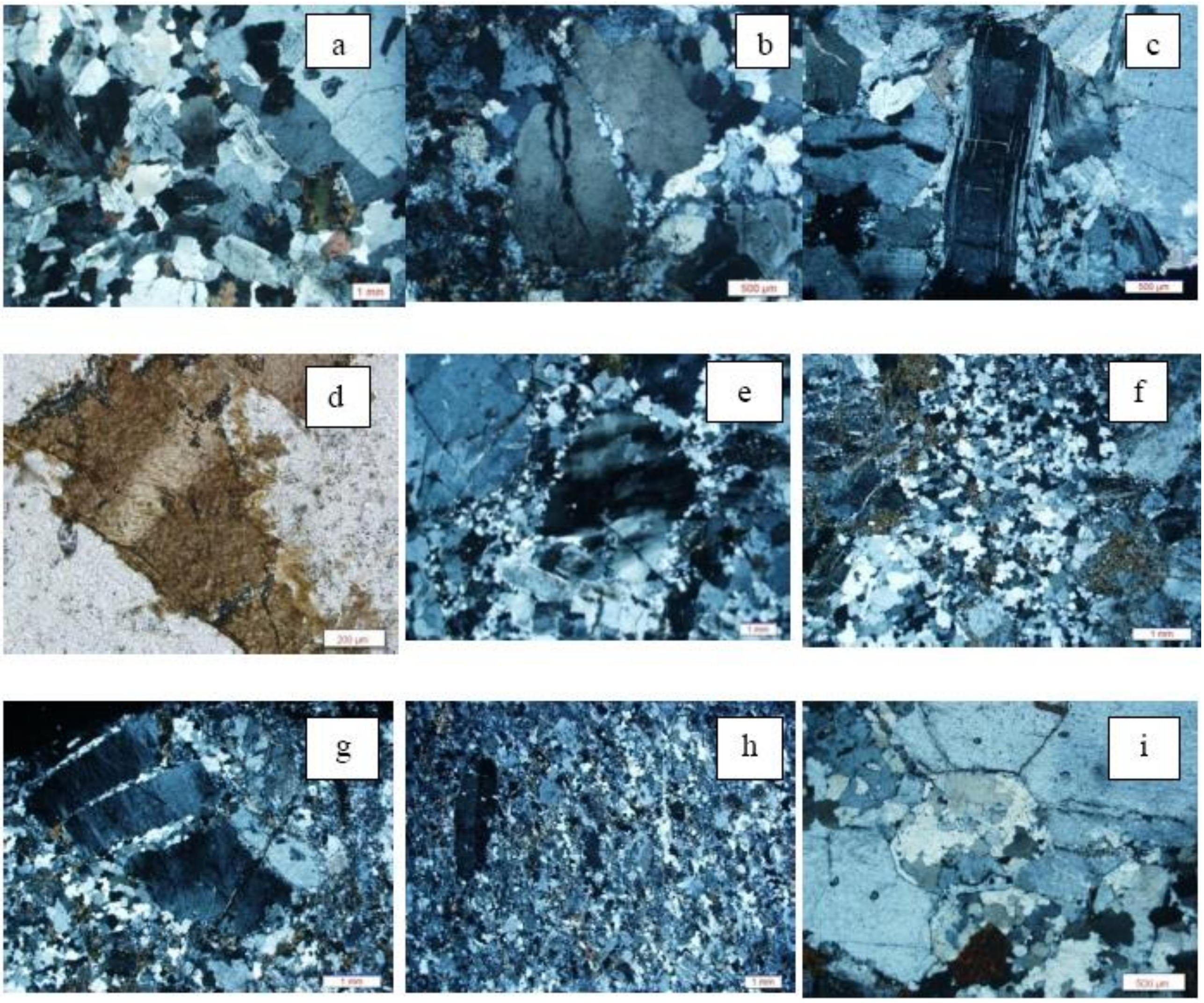

*Figure 11) Microstructures observed in the BMGP. a) magmatic (feldspar crystals are absolutely undeformed and the quartz grains display no more than minor local undulose extinction), b) sub-magmatic, c) bending twining plagioclase, d) Kink bands in biotite, c and d) show evidence of solid-state deformation at high temperatures, e, f and g) show evidence of solid-state deformation at low temperatures, h) Mylonitie, i) Recrystallization and grain boundary migration of low-grade mylonitie.*

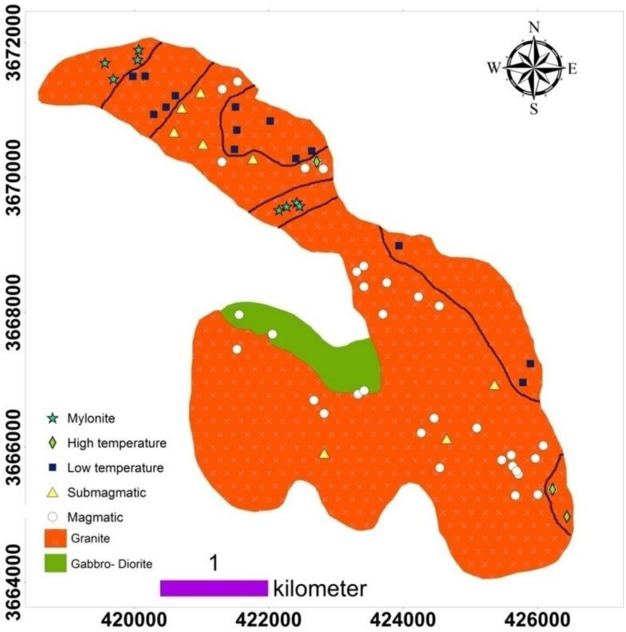


*Figure 12) Microstructural map of the BMGP.B1 Subdomain (9 Stations)*

This subdomin has been affected by tectonic stress, and shear zones which developed mylonitic fabrics. The lowest magnetic susceptibility of subdomain B1 is 5 µSI (correspond to leucogranite station) and the highest value is 421 µSI for station 56 (alkali feldspar granite). All stations have an oblate magnetic ellipsoid. Magnetic lineations mainly show north trends with low plunges.

*B2 Subdomain (8 Stations)*

The rocks of subdomain B2 are alkali feldspar granite in composition with magmatic and submagmatic microstructures. The mean magnetic susceptibility is 299 µSI. Magnetic lineations generally trend to south and have low plunges.

*Figure 13. pictures from The deformation in N and NW parts of the BMGP attributed to shear zones and faults. Attention to S and C plans in small scale dextral shear zone in these areas.*

*B3 Subdomain (13 Stations)*

The lithological composition of this subdomain is mostly alkali feldspar granite, and for one station is leucogranite showing low temperature solid state microstructure. The highest susceptibility is 188 and lowest Km is 50 μSI (mean at 124 μSI). In respectively for station 32 (alkali feldspar granite) and station 31 (leucogranite).

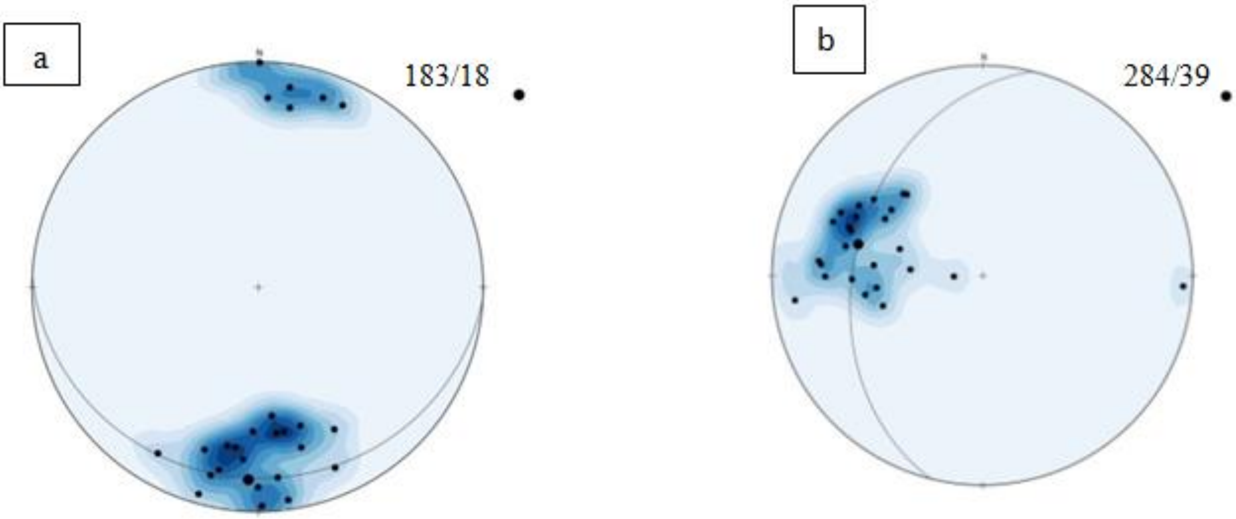


*Figure 14a) lineations and (b) the best pole of magnetic foliations in A domain.*

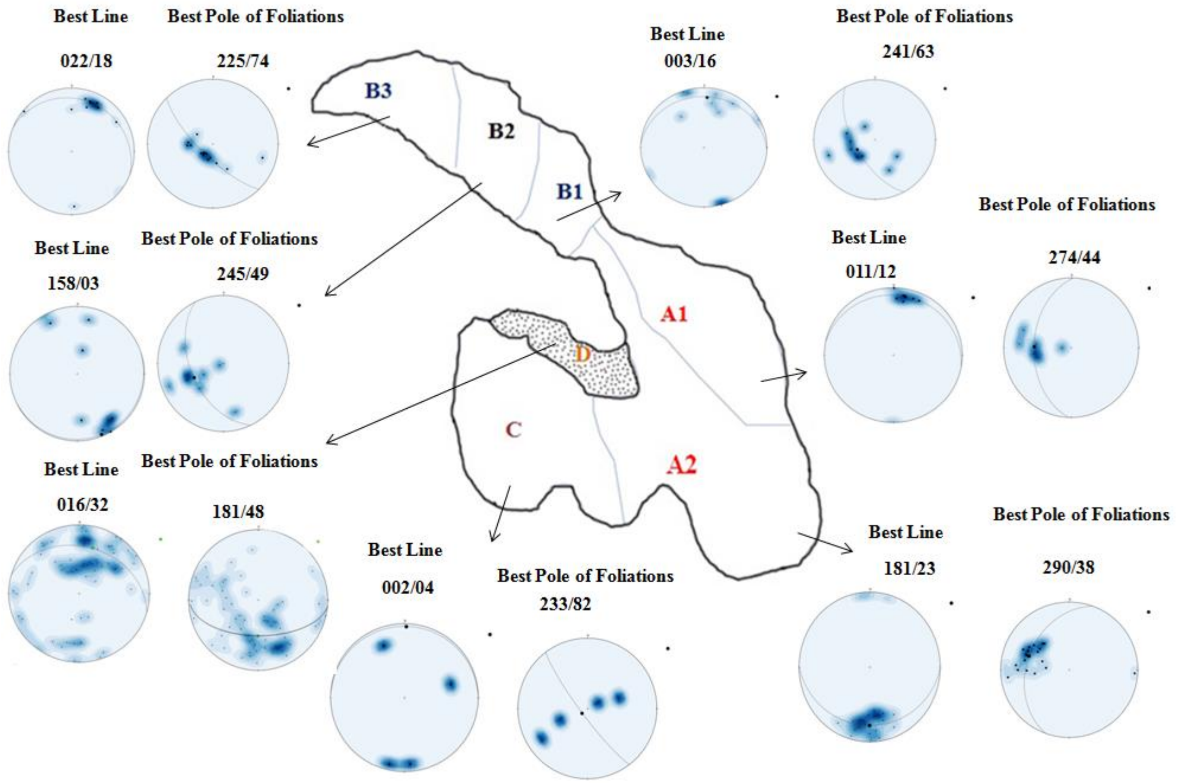


*Figure 15- Four domains of BMGP as defined from the magnetic lineations and foliations. Domain A is divided into 2 subdomains and domain B is also divided into 3 subdomains.*

### 5.1.3- C Domain (4 stations)

This small domain consists of fine grain granites. These rocks show granular texture and magmatic microstructures. The magnetic susceptibility ranges from 116 to133 μSI (mean ~122 μSI). Magnetic lineations have mean trend/plunge at 002°/04°, and the best pole of foliation has mean at 233°/82° (Fig. 17). The anisotropy percentages (P%) reaches up to 3%, and shape parameter (T) in domain for three stations are oblate and for one station it is prolate (station 24).

### 5.1.4- D Domain (3 stations)

Domain D covers the southern part of the BMGP. The rock-type are the gabbro-diorite in compositon with purely magmatic microstructure. This domain has the highest magnetic susceptibility values in the study pluton ranged from 545 to 1109 μSI (mean ~769 μSI). Lineations have mean trend/plunge of 016°/32°, and the best pole of foliation is 181°/48° (Fig. 18). The P% values are mostly less than 3%.

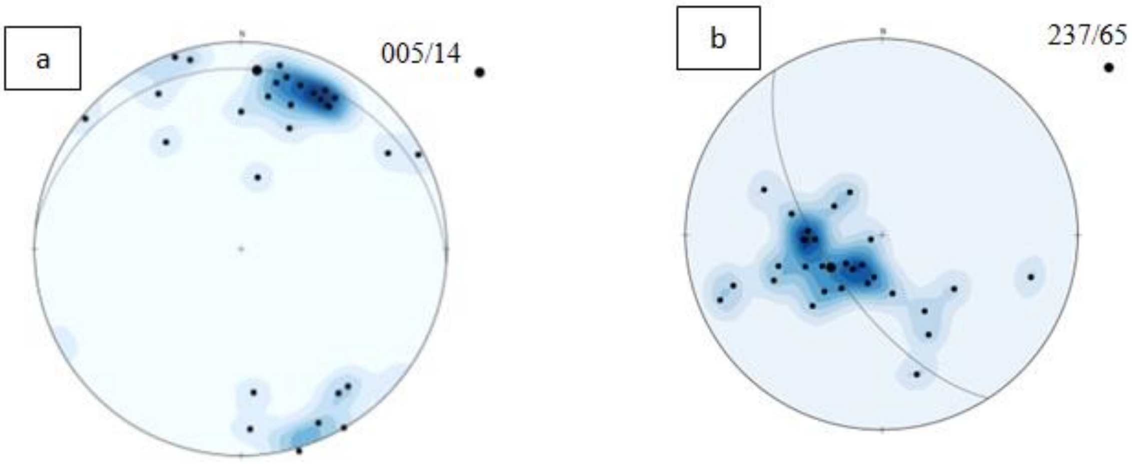


*Figure16a) lineations and b) the best pole of magnetic foliations of B domain.*

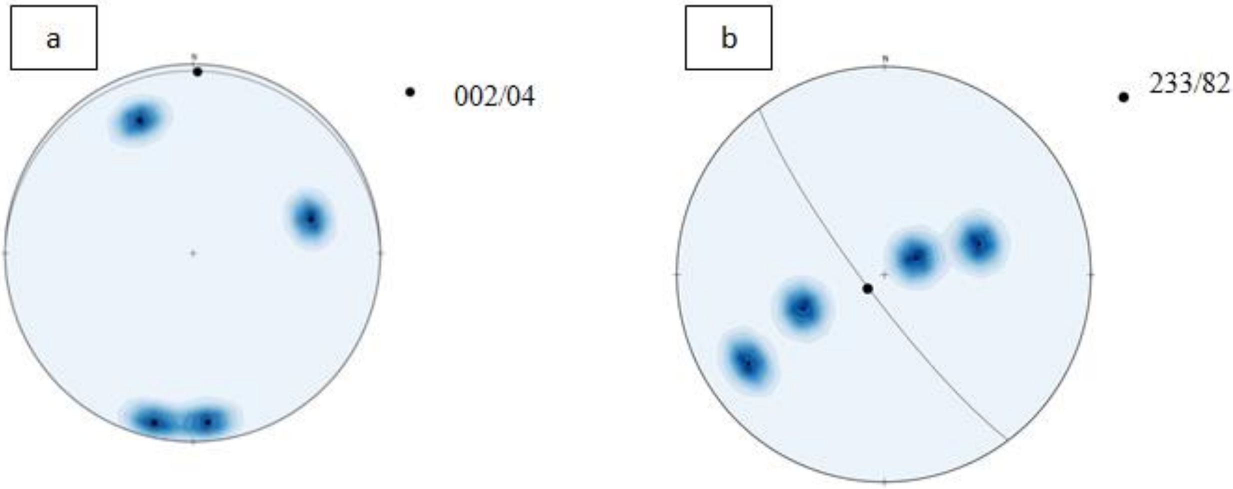


*Figure 17a) lineations and b) the best pole of magnetic foliation of C domain.*

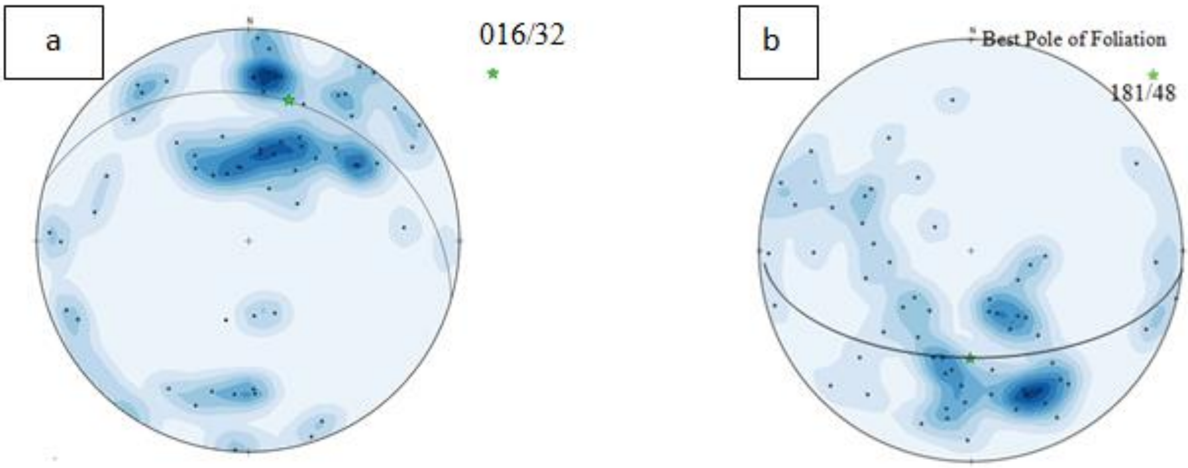


*Figure 18a) lineations and b) the best pole of magnetic foliation of D domain.*

**5.2- Model of Emplacement**

Structural setting of most Sanandaj-Sirjan plutons is an extensional environment created in related to a transpression regime duo to continue convergence between Iran and Arabia plates (Mohajjel and Ferguson, 2000). Based on Castro (1986), Mohajjel and Ferguson (2000) emphasized that dextral shear zones made a sigmoid place for emplacement of most Sanandaj-Sirjan plutons.

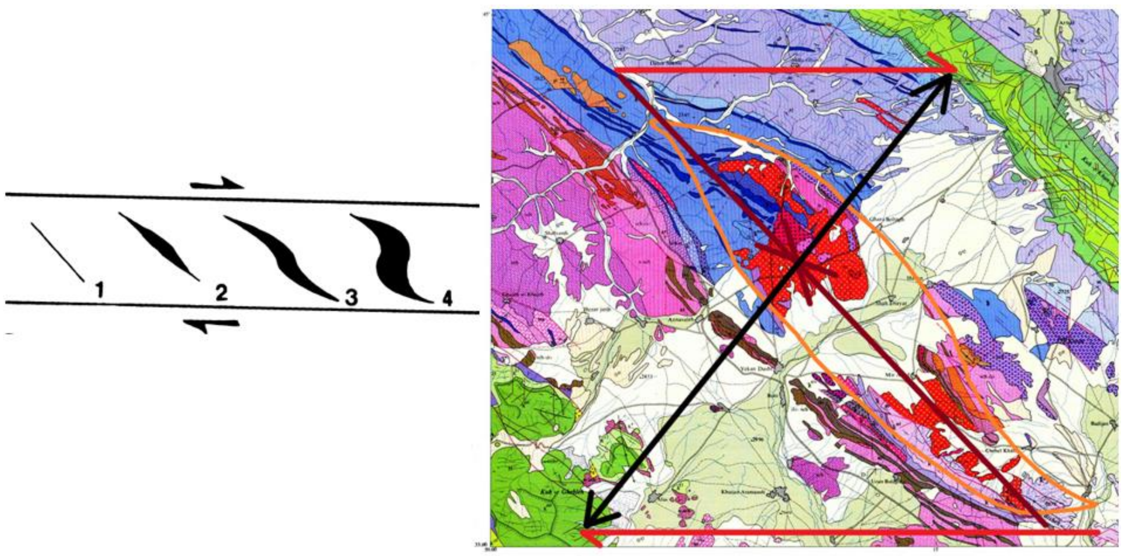


*Figures 19a) Casteo model, b) schematic picture of created extensional Basin for emplacement of the BMGP.*

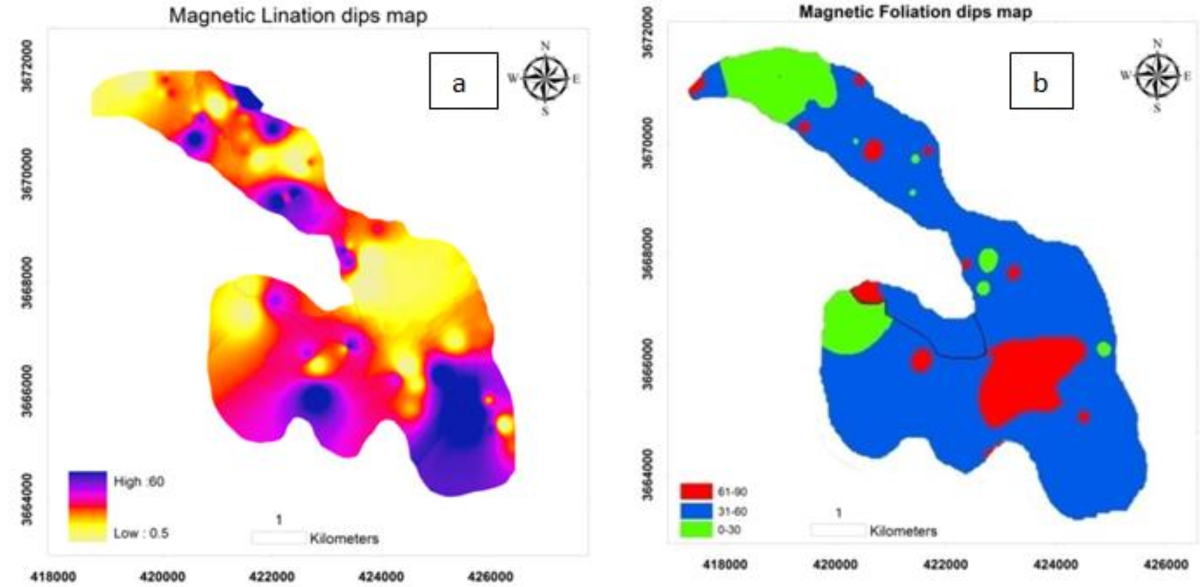


*Figure 20a) Map of variation magnetic lineation dips, b)magnetic foliation dip map.*

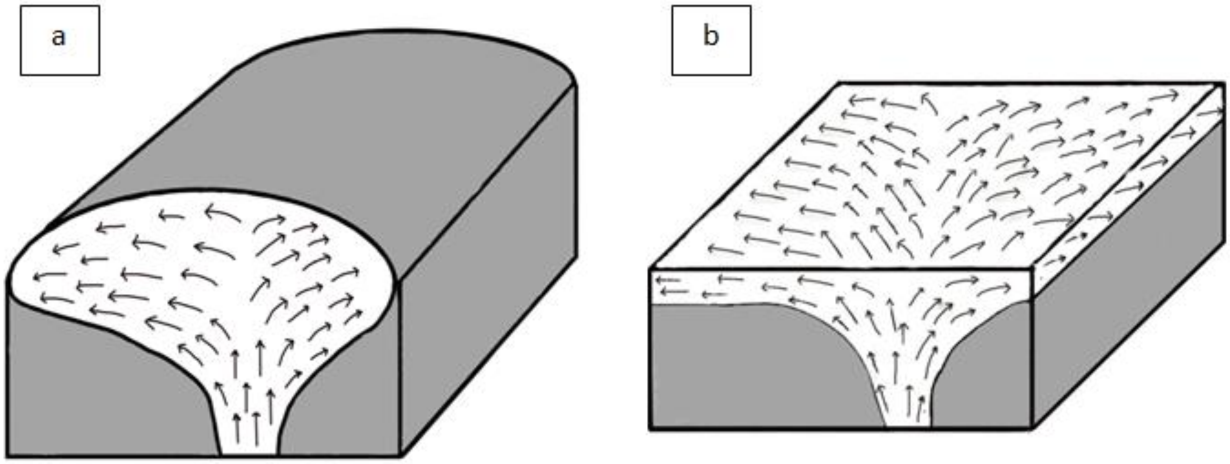


*Figure 21a) Schematically model of the emplacement mechanism of the BMGP analogous a large sill, b) block diagram of a. according to the present erosional level.*

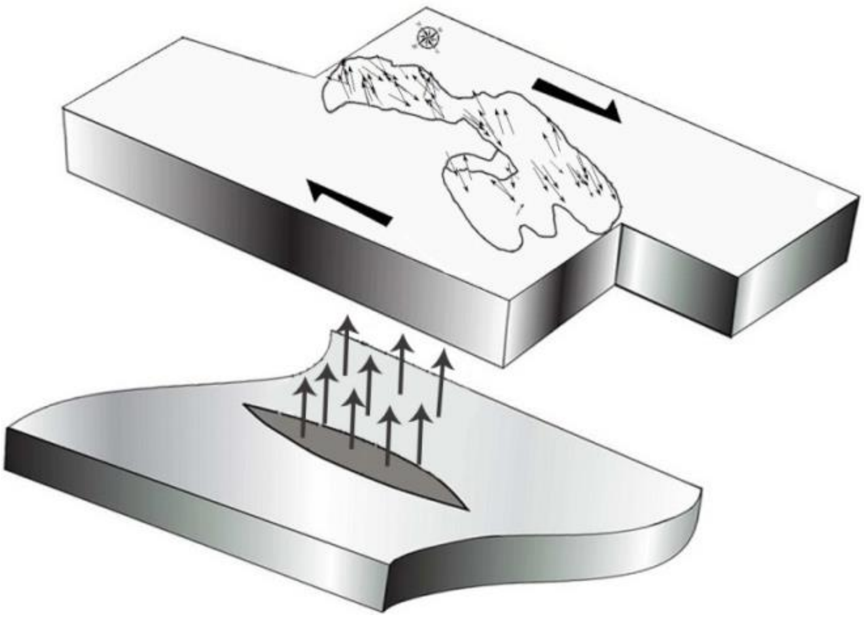

*Figure 22) A schematic picture of the emplacement of BMGP.*

This model can be adapted to the Bouin-Miandasht pluton, which consists with magnetic fabric studies, via considering the below points:

(A) The morphological shape of the studied pluton (Fig 19); (B) Distribution of magnetic lineations in two different directions: the Northeast and the Southwest (Fig. 5), (C) a suitable mechanism that is able to create an open space with curvilinear structural elements. Low plunges of magnetic lineations (Fig. 20a) and low dip foliations (Fig. 20b) suggest that the parent magma of the Bouin- Miandasht pluton was emplaced as a large sill (Fig. 21). The pluton emplacement was done in an extensional environment of a dextral shear zone (Fig. 19) created by a transpression regime (Fig. 22).

## 4-Conclusions

Magmatic microstructures are present in most parts of the The BMGP, this pluton also represents low and high temperature solid-state microstructures. Low temperature solid state microstructures present in the north and northwest parts of the pluton corresponding to shear zones and faults. The elongated shape of the pluton (like the other plutons of SSZ), low plunges of magnetic lineations and low dip foliations defined on the base of magnetic parameters suggest that the parent magma of the Bouin- Miandasht granitoid was emplaced as a large sill in a dextral shearing zone. Dextral shearing zones was created by convergence Iran and Arabia plates and made a suitable place for the emplacement of this magma during middle Jurassic.

**Acknowledgments:**

The authors would like to thank Dr. N. Georgiev, Dr. N. Théophile, Dr. F. Karelland and Dr. H. Alimohammadian for their appreciate comments which help us to improve manuscript. They also thank Dr. M. Rezaei Kahkhaei and Mr. R. Sarizan for their kind and careful comments.

**References:**

Agard, P., Omrani, J., Jolivet, L., Mouthereau, F. 2005. Convergence history across Zagros (Iran): Constraints from collisional and earlier deformation, International Journal of Earth Sciences: 4, 401–419.

Ahadnejad, V., Valizade, M., Deevsalar, R., Rezaei-Kahkhaei, M. 2011. Age and geotectonic position of the Malayer granitoids: Implication for plutonism in the Sanandaj–Sirjan zone, W iran. Neues Jahrabuch fur Geologie und Palantologie: 261, 61–75.

Ahmadi-Khalaji, A., Esmaely, D., Valizade, M. V., Rahimpour-Bonab, H. 2007. Petrology and geochemistry of the granitoid complex of Boroujerd, Sanandaj-Sirjan zone, western Iran. Journal of Asian Earth Sciences: 29, 859–877.

Balsley, J. R., Buddington, A. F. 1960. Magnetic susceptibility anisotropy and fabric of some Adirondack granites and orthogneiss. American Journal of Science: 258-A, 6–20.

Benn, K., Cruden, A. R., Sawyer, E. W. (Eds.) 1998. Extraction, transport and emplacement of granitic magmas. Journal of Structural Geology: 20 (9/10).

Berberian, M., King, G. C. P. 1981. Toward a paleogeography and tectonic evolution of Iran. Canadian Journal of Earth Science: 18, 210–265.

Borradaile, G. J., Henry, B. 1997. Tectonic applications of magnetic susceptibility and its anisotropy. Earth Science Reviews: 42, 49–93.

Borradaile, G. J., Jackson, M. 2004. Anisotropy of magnetic susceptibility (AMS): magnetic petrofabrics of deformed rocks. The Geology Society London: 238, 299–360.

Bouchez, J. L. 2002. Magnetic susceptibility anisotropy and fabrics in granites. Earth and Planetary Science Letters: 330, 1–14.

Bouchez, J. L. 1997. Granite is never isotropic: an introduction to AMS studies in granitic rocks. In: Bouchez, J. L., Hutton, D. H.W., Stephens, W. E. (Eds.), Granite: from segregation of melt to emplacement fabrics. Petrology and Structural Geology: 8, 95–112.

Bouchez, J. L., Gleizes, G., Djouadi, T., Rochette, P. 1990. Microstructure and magnetic susceptibility applied to emplacement kinematics of granites: the example of the Foix pluton (French Pyrenees). Tectonophysics: 184, 157–171.

Bouchez, J. L., Guillet, P., Chevalier, F. 1981. Structures d'écoulement liés à lami seen place du granite de Guérande (Loire Atlantique, France). Bulletin de la Société Géologique de France 7/XXIII, 387–399.

Cañón-Tapia, E., Walker, G. P. L., Herrero-Bervera, E. 1996. The internal structure of lava flows-insights from AMS measurements: I—Nearvent a'a. Journal of Volcanology and Geothermal Research: 70, 21–36.

Castro A. 1986. Structural pattern ascent model in the Central Extremadura batholith, Hercynian belt, Spain, Journal of Structural Geology: 8, 633–645.

Clemens, J. C. 1998. Observations on the origins and ascent mechanisms of granitic magmas. Journal of the Geological Society of London: 155, 843–851.

Cloos, E. 1932. Structural survey of the granodiorite south of Mariposa, California. American Journal of Science: 23, 289–304.

Cloos, E. 1931. Der Sierra Nevada Pluton. Geologische Rundschau: 22, 372–384.

D’Lemos, R. S., Brown, M., Strachan, R. A. 1992. Granite magma generation, ascent and emplacement within a transpressional orogen. Journal of the Geological Society: 149, 487–490.

Eftekharnejad, J. 1981. Tectonic division of Iran with respect to sedimentary basins. Journal of Iranian Petroleum Society: 82, 19–28.

Ferré, E. C. E., Hernandez, F., Teyssier, Ch.,Jackson, M. 2004. Paramagnetic and ferromagnetic anisotropy of magnetic susceptibility in migmatites: measurements in high and low fields and kinematic implications. Geophysical Journal International: 157, 1119–1129.

Ghasemi, A., Talbot, C. J. 2006. A new tectonic scenario for the Sanandaj-Sirjan Zone (Iran). Journal of Asian Earth Sciences: 26, 683–693.

Ghasemi, H. 1992. Investigation of petrology and geology of metamorphic and igneous rocks of the Bouin-Miandasht pluton (SE Aligoudarz). MSc thesis, University of Tehran, Tehran, Iran, 180.

Graham, J. W. 1954. Magnetic susceptibility anisotropy: an unexploited petrofabric element. Geological Society of America Abstract Program: 65, 1257–1258.

Guineberteau, B., Bouchez, J. L., Vigneresse, J. L. 1987. The Mortagne granite pluton (France) emplaced by pull-apart along a shear zone: structural and gravimetric arguments and regional implication. Geological Society of America Bulletin: 99, 763–770.

Hargraves, R. B., Johnson, O., Chan, C. Y. 1991. Distribution anisotropy: the cause of AMS in igneous rocks? Geophysics Research Letters: 18, 2193–2196.

Hrouda, F. 1982. Magnetic anisotropy of rocks and its application in geology and geophysics. Geophysical Surveys: 5, 37–82.

Hutton, D. H. W., Dempster, T. J., Brown, P. E., Becker, S.D. 1990. A new mechanism of granite emplacement: intrusion in active extensional shear zones. Nature: 343, 452–455.

Hutton, D. H. W., Reavy, R. J. 1992. Strike-slip tectonics and granite petrogenesis. Tectonics: 11, 960–967.

Jelinek, V. 1981. Characterization of the magnetic fabrics of rocks. Tectonophysics: 79, 63–67.

Khan, M. A. 1962. Anisotropy of magnetic susceptibility of some igneous and metamorphic rocks. Journal of Geophysical Research: 67, 2873–2885.

Masoudi, F. 1997. Contact metamorphism and pegmatite development in the region SW of Arak, Iran. PhD thesis. University of Leeds, 200.

McCAll, G. J. H. 2002. A summary of the geology of the Iranian Makran. – In: Cliff P. D., Kroon, D., Gaedecke, C. and Craig, J. (Eds.): The tectonics and climatic evolution of the Arabian Sea region. Geological Society of London Special Publication: 195, 147–204.

Mohajjel, M., Fergusson, C. L., Sahandi, M. R. 2003. Cretaceous-Tertiary convergence and continental collision, Sanandaj-Sirjan Zone, western Iran. Journal of Asian Earth Sciences: 21: 397–412.

Mohajjel, M., Fergusson, C. L. 2000. Dextral transpression in Late Cretaceous continental collision, Sanandaj-Sirjan zone, western Iran.

Journal of Structural Geology: 22, 1125–1139.

Moritz, R., Ghazban, F., Signer, B. S. 2006. Eocene gold ore formation at Muteh, Sanandaj-Sirjan tectonic zone, Western Iran: a result of late-stage extension and exhumation of metamorphic basement rocks within the Zagros orogen. Economic Geology: 101, 1497–1524.

Paterson, S. R., Vernon, R. H., Tobish, O. T. 1989. A review of criteria for the identification of magmatic and tectonic foliations in granitoids. Journal of Structural Geology: 11, 349–363.

Rochette, P., Jackson, M., Aubourg, C. 1992. Rock magnetism and the interpretation of anisotropyof magnetic susceptibility.Reviews of Geophysics: 36, 209–226.

Saki, S. 2014. Investigation of emplacement mechanism of Bouin-Miandasht granitoidic pluton by using anisotropy of magnetic susceptibility (AMS) method, MSc thesis, University of Shahrood, Shahrood, Iran, 230.

Tarling, D. H. Hrouda, F. 1993. The magnetic Anisotropy of rocks, Chapman and Hall, London. 217p .

Tauxe, L., Gee, J. S., Staudigel, H. 1998. Flow directions in dikes from anisotropy of magnetic susceptibility data: the bootstrap way. Journal of Geophysical Research-Solid Earth: 103, 17775–17790.

Zhang, Sh., Canon-Tapia, E., Walderhaug, H. J. 2011. Magnetic fabric and its significance in the Sills and lava flow from Taimyr fold-belt, Arctic Siberia. Tectonophysics: 505, 68–85.